

Detailed mechanism and molecular weight dependence of thermal degradation of polyisobutylene

Takashi Sawaguchi* and Manabu Seno

Department of Industrial Chemistry, College of Science and Technology, Nihon University, Kandasurugadai, Chiyoda-ku, Tokyo 101, Japan

(Received 16 February 1996; revised 25 March 1996)

The products of thermal degradation of polyisobutylene are successfully simulated according to a radical chain reaction model including diffusion-controlled termination reactions of primary and tertiary terminal macroradicals ($R_p \cdot$ and $R_t \cdot$) and volatile small radical ($S \cdot$). The model proposed consists of the following three steps: (1) end and random initiation reactions, (2) depropagation consisting of depolymerization and intramolecular and intermolecular hydrogen abstractions followed by β scissions, and (3) diffusion-controlled termination consisting of bimolecular reactions between respective macroradicals and vaporization of volatile radicals. The molecular weight (M) dependencies of rates of the end initiation and termination are evaluated by M^{-1} and M^{-n} , respectively. Assuming that the reaction occurs competitively under steady state conditions regarding the respective radicals, their concentrations could be approximately expressed as a function of M . The observed values of the compositions of the studied components of the volatile oligomers and functional groups of the nonvolatile oligomers formed by the degradation at 300°C, are consistently traced by simulation using the above model when the value of n is about 2 for the self-diffusional motion of the reacting radical in the molten polymer matrix. Rates of decreases in concentration are of the order: $S \cdot > R_p \cdot \gg R_t \cdot$. This results from an increase in the rate of termination with a decreasing molecular weight of the matrix as the reaction proceeds. Copyright © 1996 Elsevier Science Ltd.

(Keywords: thermal degradation; polyisobutylene; simulation)

INTRODUCTION

Many attempts have been intensively made to elucidate the effect of polymer dynamics on polymer reactions, being supported by recent theoretical and experimental studies of polymer physics¹. The diffusion-controlled termination in free-radical polymerization was especially analysed based on an interpolymer reaction model², and the effects of diffusion of the reacting polymer molecules as well as their molecular weight and solvent were made clear³. Mita and Horie⁴ reviewed the effects of molecular weight of polymer molecules and the translational diffusion of polymer segments on polymer reactions in solution, and the effect of secondary transition on polymer reactions in bulk, but little is known about these effects on polymer reactions in melt.

The molecular weight would affect strongly the polymer reaction in melt such as thermal degradation of polymers⁵, although this is not yet fully understood. The rate of random scission in the thermal degradation of anionically prepared polystyrene increases with an increasing initial molecular weight of the sample⁶ and this result could be interpreted to be due to an increase in macroradical concentration based on the diffusion-controlled termination model⁴. In a series of the present

studies⁷, we attempt to elucidate the effect of molecular weight on the thermal degradation of polyisobutylene from structural and kinetic analyses of the products. It was observed that the values of composition ratios between interesting components in the volatile and nonvolatile oligomers decrease clearly with an increasing time^{7b,e}, and the decrease in the composition ratios results from a decrease in molecular weight of the matrix during the degradation^{7c,e}. By a preliminary kinetic approach to the elementary reactions, it was deduced that the decrease in molecular weight of the matrix leads to a decreasing concentration ratio ($[R_p \cdot]/[R_t \cdot]$) (see Appendix for meanings of the symbols) of two types of macroradicals, due to an increase in the rate of diffusion controlled termination. Moreover, similar power laws of the molecular weight dependence of the radical concentration ratio were obtained separately for the volatile and the nonvolatile oligomers^{7c,e}; that is, similar behaviours of the decrease in the ratio $[R_p \cdot]/[R_t \cdot]$ during the degradation were observed on the different elementary reactions for formation of the different products.

In this paper, we discuss the composition ratios between the components of interest of the products formed by the degradation traced by computer simulation of a total reaction model including diffusion-controlled termination, and the effect of molecular weight on the radical concentration.

*To whom correspondence should be addressed

EXPERIMENTAL

Sample, apparatus and procedure

The polyisobutylene sample and the experimental procedure were described in detail elsewhere^{7a}. Molecular weight characteristics of the purified polyisobutylene are $M_n = 2.5 \times 10^5$ and $M_w/M_n = 2.50$. One gram of the sample was used for each degradation experiment at 300°C. After the degradation reaction the polymer residue in the reaction flask was dissolved in 10 cm³ of chloroform and the solution was reprecipitated by dropping it into 50 cm³ of acetone to remove a small amount of the semi-volatile oligomers with a relatively low volatility. The reprecipitates were termed the nonvolatile oligomers and analysed after vacuum drying under heating. The composition of the nonvolatile and semi-volatile oligomers was determined with g.p.c. analysis.

Analysis

The 400 MHz ¹H n.m.r. spectra were measured with a Jeol JNM-GX400 spectrometer operating at 399.65 MHz and room temperature with an internal lock. Sample concentrations were approximately 10%

(w/v) in chloroform-*d*₁. Tetramethylsilane (TMS) was used as an internal standard and the 5 mm-diameter sample tubes were used. Spectral widths were 4.5 kHz, and 65 536 data points were accumulated in a JEC 32 computer. In the quantitative measurement^{7d}, the pulse width of 90° (approximately 11.7 μs) and the pulse repetition time of 37.281 s were adopted. A typical measurement was performed for about 10–45 h. The signal intensities in the spectra were measured by a weighing method. The composition of the functional groups was determined from the intensities of signals of the corresponding methyl protons^{7d}.

The molecular weight dispersion (M_w/M_n) was measured by an analytical g.p.c. (Toyo Soda HLC-802 UR) using a stainless-steel column of TSK-GEL (2 · HMG6 + H4000HG8 + H2000HG8). The data were calibrated with the standard polystyrene. M_n was determined by the following equation⁸ using the limiting viscosity number measured at 30°C in toluene: $[\eta] = 3.71 \times 10^{-4} P^{0.75}$, where $[\eta]$ is the limiting viscosity number (lg⁻¹) and P is the number average degree of polymerization determined by the osmotic pressure method.

Gas chromatography of the volatile oligomers was recorded on a Shimadzu GC-8A gas chromatograph

Table 1 Changes in volatilization and composition ratios of oligomers of interest in the volatile oligomers with the thermal degradation of polyisobutylene ($M_n=2.50 \times 10^5$) at 300°C

Time (min)	M_n^a $\times 10^{-3}$	C^b wt%	$C^{c'}$ wt%	Trimers ($n = 1$)				Tetramers ($n = 2$)			
				$\frac{[TTD]_p}{[TVD]_p}$	$\frac{[TTD]_t}{[TVD]_t}$	$\frac{[TVD]_p}{[TVD]_t}$	$\frac{[TTD]_p}{[TTD]_t}$	$\frac{[TTD]_p}{[TVD]_p}$	$\frac{[TTD]_t}{[TVD]_t}$	$\frac{[TVD]_p}{[TVD]_t}$	$\frac{[TTD]_p}{[TTD]_t}$
15	35.0	4.1	4.2	2.05	1.39	85.0	125	1.93	1.18	20.3	33.2
15	31.8	4.3	4.4	2.05	1.35	67.1	102	1.94	1.29	17.5	26.2
20	26.4	4.5	5.0	2.07	1.15	62.1	112	1.89	0.98	17.7	34.1
25	19.1	6.3	7.0	2.22	1.35	52.7	86.6	2.11	1.38	15.8	24.2
30 ^d	15.0	6.3	9.9	2.19	1.06	32.4	66.6	1.96	1.36	11.8	17.0
60 ^d	13.3	6.9	10.8	2.18	1.10	26.0	51.5	1.95	1.40	11.3	15.7
120 ^d	8.97	11.5	17.1	2.22	1.14	16.7	32.6	1.99	1.61	8.81	10.9
140 ^d	8.47	12.6	21.5	1.98	1.16	16.5	28.2	2.23	1.43	7.93	12.4
180 ^d	7.02	16.0	24.6	2.22	1.13	13.5	26.6	1.95	1.48	6.84	9.02
300 ^d	5.52	23.6	32.4	2.18	1.08	8.93	18.0	2.14	1.48	4.48	6.45

Pentamers ($n = 3$)				Hexamers ($n = 4$)				Heptamers ($n = 5$)			
$\frac{[TTD]_p}{[TVD]_p}$	$\frac{[TTD]_t}{[TVD]_t}$	$\frac{[TVD]_p}{[TVD]_t}$	$\frac{[TTD]_p}{[TTD]_t}$	$\frac{[TTD]_p}{[TVD]_p}$	$\frac{[TTD]_t}{[TVD]_t}$	$\frac{[TVD]_p}{[TVD]_t}$	$\frac{[TTD]_p}{[TTD]_t}$	$\frac{[TTD]_p}{[TVD]_p}$	$\frac{[TTD]_t}{[TVD]_t}$	$\frac{[TVD]_p}{[TVD]_t}$	$\frac{[TTD]_p}{[TTD]_t}$
2.05	1.18	18.4	35.7	2.15	1.02	10.9	23.1	1.90	1.12	10.2	17.4
1.99	1.14	14.3	25.0	2.18	1.03	8.74	18.6	2.32	1.16	7.09	14.3
1.86	0.79	14.4	33.9	2.20	1.10	10.1	20.1	2.10	1.16	9.13	16.6
1.85	1.05	13.5	23.7	2.12	1.37	11.7	18.2	2.26	1.16	7.51	14.6
2.02	1.17	10.9	18.8	2.11	1.04	7.79	15.7	1.96	1.17	7.35	12.3
2.00	1.19	8.42	14.2	2.16	1.02	6.12	13.0	2.08	1.09	5.84	11.1
2.13	1.45	5.84	8.60	2.08	1.10	4.08	7.71	2.14	1.28	3.73	6.27
1.90	1.02	5.55	10.4	2.29	1.01	5.03	11.4	2.17	1.25	4.61	8.01
2.15	1.33	4.56	7.38	2.17	1.20	3.78	6.84	2.12	1.30	3.63	5.93
2.09	1.31	3.71	5.91	2.15	1.63	3.78	4.98	2.09	1.45	2.07	2.99

^a By limiting viscosity number measurements

^b Volatilization

^c $C + C'$ (semi-volatile oligomers)

^d From ref. 7b, c

equipped with a flame-ionization detector and a fused silica capillary column (50 m × 0.35 mm i.d.) consisting of OV-1. The instrumental conditions were described elsewhere^{7b}. The composition ratios for the respective oligomers were obtained by the relative ratios of the peak intensities, and were measured with a digital integrator without calibration.

RESULTS AND DISCUSSION

Characterization of the degradation

In previous papers^{7a,d}, both the volatile oligomers and the nonvolatile oligomers isolated from the polymer residue obtained by thermal degradation of polyisobutylene were precisely characterized. The results clearly show that most of the products are derived from $R_p \cdot$ and $R_t \cdot$ and $S \cdot$ in the depropagation step of the radical chain mechanism.

The results of thermal degradation at 300°C are given in Table 1, where M_n of the nonvolatile oligomers, the yield of volatiles C and the composition ratios between respective terminal mono-olefins of each volatile oligomer are listed as functions of reaction time. The yield of volatiles increases and then the polymer residue constituting the reaction media decreases as the degradation proceeds. The volatiles consist of the monomeric compounds (10–30 wt%), mainly isobutylene monomer, and the volatile oligomers (90–70 wt%) ranging from dimers to dodecamers. Isobutylene monomer is formed by depolymerization (direct β scission) of $R_p \cdot$ and $R_t \cdot$. The volatile oligomers consist mainly of four types of mono-olefins [(TTD)_p, (TVD)_p, (TTD)_t and (TVD)_t],

which are formed by the intramolecular hydrogen abstraction (back-biting) of $R_p \cdot$ and $R_t \cdot$ and the subsequent β scission at the inner position of the main chain. According to a kinetic approach to back-bitings, the ratios [TTD]_p/[TVD]_p and [TTD]_t/[TVD]_t given in Table 1 correspond to those between the abstraction rates of different types of hydrogens (CH_2 and CH_3) of the same type of macroradicals ($R_p \cdot$ or $R_t \cdot$), respectively, and could be expressed by the kinetic rate constant ratio^{7b}. These ratios have different values from trimers to heptamers, but remain nearly constant during the degradation. This observed tendency agrees fairly well with the kinetic expectation. On the other hand, the ratios [TTD]_p/[TTD]_t and [TVD]_p/[TVD]_t correspond to those between the abstraction rates of the same type hydrogen (CH_2 or CH_3) of different macroradicals ($R_p \cdot$ and $R_t \cdot$), respectively, and could be expressed by an integrated radical concentration ratio [$R_p \cdot$]/[$R_t \cdot$], according to the kinetic analysis^{7b}. The observed values (Table 1) are different for each oligomer and decrease clearly with reaction time. The decrease in these ratios with time is evidently due to a decrease of the ratio [$R_p \cdot$]/[$R_t \cdot$]^{7b}.

Table 2 shows the results of characterization of the nonvolatile oligomers obtained under the same conditions as Table 1. Although the M_n value of the nonvolatile oligomers decreases to 5500 for 300 min, the M_w/M_n value keeps a nearly constant value of 2. The functionality of functional groups (*t*-Bu, *i*-Pr, TVD, TTD and NTTD) is defined as the average number of a given functional group per molecule, and calculated by the following equation, assuming all the nonvolatile

Table 2 Changes in molecular weight characteristics, composition and functionality of respective end groups and double bonds in the nonvolatile oligomers with thermal degradation of polyisobutylene ($M_n = 2.50 \times 10^5$) at 300°C

Time (min)	C^a (wt%)	$M_n^b \times 10^{-3}$	M_w/M_n^c	Composition ^d (mol%)					Functionality ^j						
				[<i>i</i> -Pr] ^e	[<i>t</i> -Bu] ^f	[TTD] ^g	[TVD] ^h	[NTTD] ⁱ	f_{i-Pr}	f_{t-Bu}	f_{TTD}	f_{TVD}	f_{NTTD}	f_t^k	f_{in}^l
0 ^m	0.0	250	2.50	0.00	50.00	25.00	25.00	0.00	0.000	1.000	0.500	0.500	0.000	1.00	1.00
15	4.1	35.0	2.20	0.33	24.23	45.50	22.04	7.90	0.007	0.526	0.992	0.479	0.172	1.47	1.64
15	4.3	31.8	2.22	0.40	23.52	46.02	21.91	8.15	0.009	0.512	1.00	0.477	0.177	1.48	1.66
20	4.5	26.4	2.18	0.45	22.55	46.67	21.68	8.65	0.010	0.494	1.02	0.475	0.189	1.50	1.69
25	6.3	19.1	2.20	0.46	19.44	48.68	22.39	9.03	0.010	0.427	1.07	0.492	0.199	1.56	1.76
30 ⁿ	6.3	15.0	2.17	0.53	15.37	51.09	23.36	9.65	0.012	0.340	1.13	0.517	0.214	1.65	1.86
60 ⁿ	6.9	13.0	2.14	0.61	16.00	51.51	22.33	9.95	0.013	0.354	1.14	0.494	0.220	1.63	1.85
120 ⁿ	11.5	8.97	2.12	1.04	16.01	52.90	20.13	9.92	0.023	0.355	1.17	0.447	0.220	1.62	1.84
140 ⁿ	12.6	8.47	2.15	1.12	15.32	52.35	21.18	10.03	0.025	0.341	1.16	0.471	0.223	1.63	1.86
180 ⁿ	16.0	7.02	2.11	1.41	17.90	51.62	18.72	10.35	0.031	0.399	1.15	0.418	0.231	1.57	1.80
300 ⁿ	23.6	5.52	2.10	2.01	17.90	52.73	15.97	11.39	0.045	0.404	1.19	0.360	0.257	1.55	1.81

^a Volatilization

^b By limiting viscosity number measurements

^c Heterogeneity index of molecular weight distribution determined by g.p.c. measurements

^d $100 \times$ [each CH_3 peak intensity/total CH_3 peak intensity (*i*-Pr + *t*-Bu + TTD + TVD + NTTD)]

^e *Iso*-propyl; $(CH_3)_2CH-$

^f *Tert*-butyl; $(CH_3)_3C-$

^g Terminal trisubstituted double bond; $(CH_3)_2C=CH-$

^h Terminal vinylidene double bond; $CH_2=C(CH_3)-$

ⁱ Nonterminal trisubstituted double bond; $-(CH_3)C=CH-$

^j Average number of each functional group per molecule; $f = 2 \times$ [each functional group peak intensity]/total terminal peak intensity (*i*-Pr + *t*-Bu + TTD + TVD)

^k Average number of terminal double bonds per molecule; $f_t = 2 \times (TTD + TVD)/(i-Pr + t-Bu + TTD)$

^l Average number of total double bonds per molecule; $f_{in} = 2 \times (TTD + TVD + NTTD)/(i-Pr + t-Bu + TTD + TVD)$

^m Composition and functionalities are tentatively estimated

ⁿ From ref. 7e

oligomers are linear^{7d}

$$f = \frac{2 \times [\text{signal intensity of the functional group of interest}]}{[\text{signal intensity of all end groups (}i\text{-Pr} + t\text{-Bu} + \text{TTD} + \text{TVD})]}$$

The functionalities f_t and f_{in} in Table 2 represent average numbers of the terminal double bonds and the total double bonds per molecule, respectively. The original polyisobutylene ($M_n = 2.5 \times 10^5$) is a linear polymer having a saturated end group and a terminal double bond⁹; it is deduced from the cationic mechanism of preparation that the former is *t*-Bu and the latter is TTD or TVD with ratio of 1:1. As shown in Table 2, $f_{i\text{-Pr}}$ markedly increases, f_{TTD} and f_{NTTD} slightly increase, and $f_{t\text{-Bu}}$ and f_{TVD} change complicatedly with degradation time. Especially, the f_t value is greater than 1 and varies during the degradation. This result could be interpreted by considering the intermolecular hydrogen abstraction of $S\cdot$ followed by β scission, in addition to that of $R_p\cdot$ and $R_t\cdot$ ^{7d}. The volatile radical $S\cdot$ has not been taken into consideration hitherto.

The concentration $[P]$ of polymer in the molten polymer matrix is expressed by ρ/M^{10} . The density ρ is almost constant during the degradation, because the specific volume v_{sp} of polyisobutylene at 217°C is given by the equation¹¹, $v_{\text{sp}} = 1.225 + 32/M$, in a range of M from 3540 to 115 000. Under these conditions, the concentrations (mol cm^{-3}) of respective functional groups are expressed as

$$[t\text{-Bu}] = [P]f_{t\text{-Bu}} = \rho f_{t\text{-Bu}}/M \quad (1)$$

$$[i\text{-Pr}] = [P]f_{i\text{-Pr}} = \rho f_{i\text{-Pr}}/M \quad (2)$$

$$[\text{TTD}] = [P]f_{\text{TTD}} = \rho f_{\text{TTD}}/M \quad (3)$$

$$[\text{TVD}] = [P]f_{\text{TVD}} = \rho f_{\text{TVD}}/M \quad (4)$$

$$[\text{NTTD}] = [P]f_{\text{NTTD}} = \rho f_{\text{NTTD}}/M \quad (5)$$

Assuming the value of ρ to be 0.75 g cm^{-3} at 300°C, the molar concentrations given by equations (1) to (5) could be calculated from the observed values of functionality and M_n (Table 2). The calculated values of the molar

concentrations of the respective functional groups and their composition ratios at various degradation times are shown in Table 3. All of the concentrations, $[t\text{-Bu}]$, $[i\text{-Pr}]$, $[\text{TTD}]$, $[\text{TVD}]$ and $[\text{NTTD}]$, increase with an increasing time, owing to the decrement of M_n . Since the original polyisobutylene ($M_n = 2.5 \times 10^5$) would have a *t*-Bu and a terminal double bond consisting of TTD and TVD⁹, as described above, the initial concentrations $[P]_0$ and $[t\text{-Bu}]_0$ are to be 2.91×10^{-6} , $[\text{TTD}]_0$ and $[\text{TVD}]_0$ to be 1.46×10^{-6} , and $[i\text{-Pr}]_0 = [\text{NTTD}]_0 = 0$. The end initiation⁵ at thermally labile bonds of allylic position from the terminal double bonds (TVD and TTD) is of importance in addition to the random initiation by scission of the skeletal C–C bond¹². However, the elementary reactions to form TVD and TTD in the depropagation step occur more frequently than the initiation from TVD and TTD, due to their relatively large kinetic chain length (KCL)⁵, besides a minor contribution of the termination by disproportionation. Moreover, the changes in values of M_n and M_w/M_n (Table 2) suggest that the scission reaction of the main chain occurs at a random position of the polymer. The average number of scissions, which is estimated by $(M_{n0}/M_n) - 1$, is from about 6 to 124 for the nonvolatile oligomers. Thereby, over 86% of the end groups of these oligomers are newly formed by the scission reactions. It could be deduced from these results that the changes in concentrations of functional groups with degradation time (Table 3) do not depend on the initial concentration as well as the initiation and termination reactions, but depend mainly on the depropagation reactions.

The reasonable elementary reactions^{7d} were proposed for the formation of these functional groups; the intermolecular hydrogen abstractions of radicals give two types of on-chain macroradicals ($R_{\text{oi}1}\cdot$ and $R_{\text{oi}2}\cdot$), depending on the position (CH_3 or CH_2) of hydrogen abstraction, independent of radical type. Moreover, the hydrogen abstractions of $R_p\cdot$, $R_t\cdot$ and $S\cdot$ yield *t*-Bu, *i*-Pr and SH (volatiles), respectively. The β scission of $R_{\text{oi}1}\cdot$ occurs only at the main chain and exclusively results in the formation of TVD and $R_p\cdot$. On the other hand,

Table 3 Changes in concentration and composition ratios of respective functional groups in the nonvolatile oligomers with thermal degradation of polyisobutylene ($M_n = 2.50 \times 10^5$) at 300°C

Time (min)	Concentration ^a x 10 ⁶ (mol cm ⁻³)					$\frac{[t\text{-Bu}]}{[i\text{-Pr}]}$	$\frac{[\text{TTD}] + [\text{NTTD}]}{[\text{TVD}]}$	$\frac{[\text{TTD}]}{[\text{NTTD}]}$	$\frac{[\text{TTD}]}{[\text{TTD}] + [\text{TVD}]}$	$\frac{[\text{TTD}] + [\text{TVD}]}{[\text{TTD}] + [\text{TVD}] + [\text{NTTD}]}$
	$[i\text{-Pr}]$	$[t\text{-Bu}]$	$[\text{TTD}]$	$[\text{TVD}]$	$[\text{NTTD}]$					
0 ^b	0.000	2.91	1.46	1.46	0.00		1.00		0.50	
15	0.149	10.9	20.6	9.96	3.57	73.4	2.42	5.76	0.67	0.90
15	0.199	11.7	22.9	10.9	4.06	58.8	2.47	5.65	0.68	0.89
20	0.272	13.6	28.2	13.1	5.23	50.1	2.55	5.40	0.68	0.89
25	0.385	16.3	40.8	18.8	7.57	42.3	2.58	5.39	0.68	0.89
30 ^c	0.568	16.5	54.7	25.0	10.3	29.0	2.60	5.29	0.69	0.89
60 ^c	0.738	19.4	62.3	27.0	12.0	26.2	2.75	5.18	0.70	0.88
120 ^c	1.87	28.8	95.3	36.3	17.9	15.4	3.12	5.33	0.72	0.88
140 ^c	2.14	29.3	100	40.5	19.2	13.7	2.90	5.22	0.71	0.88
180 ^c	3.26	41.4	119	43.3	23.9	12.7	3.31	4.99	0.73	0.87
300 ^c	5.98	53.3	157	47.5	33.9	8.91	4.02	4.63	0.77	0.86

^a Calculated by the equation: $f\rho/M_n$

^b Estimated tentatively

^c From ref. 7e

the β scission of $R_{oi2}\cdot$ produces TTD and $R_p\cdot$, and NTTD and methyl radical, depending on the positions (main chain or side methyl group) of the scission.

According to the reaction model described above, the formations of functional groups of the nonvolatile oligomers were kinetically analysed, assuming the reactions competitively occur under a steady state where the concentrations of the on-chain macroradicals ($R_{oi1}\cdot$ and $R_{oi2}\cdot$) are kept low and constant. The molar concentrations of respective functional groups formed for a given time were obtained by integration^{7c}. The mechanism of formation of these functional groups is examined by analysing the observed values of ratios between the compositions of respective functional groups (Table 3) according to the kinetic equations giving the corresponding ratios^{7c}. The ratio $[t\text{-Bu}]/[i\text{-Pr}]$ is expressed as a product of the ratio of the rate constants and the ratio of macroradical concentrations ($[R_p\cdot]/[R_t\cdot]$). Thus, a change of $[t\text{-Bu}]/[i\text{-Pr}]$ reflects that of the macroradical concentration ratio during the degradation. On the other hand, the ratio $([TTD] + [NTTD])/[TVD]$ is expressed in terms of the ratios of the abstraction rates of different types of hydrogens (CH_2 and CH_3) of $R_p\cdot$, $R_t\cdot$ and $S\cdot$. The ratio $[TTD]/[NTTD]$ is expressed by only the rate constant ratio. The ratios $[TTD]/[TVD]$ and $([TTD] + [TVD])/([TTD] + [TVD] + [NTTD])$ given in Table 3 are described later.

As shown in Table 3, the value of $[t\text{-Bu}]/[i\text{-Pr}]$ decreases clearly with the degradation time. This tendency is consistent with that obtained for the corresponding composition ratios for the volatile oligomers concerning the ratio $[R_p\cdot]/[R_t\cdot]$ ^{7b}. The decrease in $[t\text{-Bu}]/[i\text{-Pr}]$ with time evidently results from a decreasing macroradical concentration ratio ($[R_p\cdot]/[R_t\cdot]$). This leads to the conclusion^{7b,c} that the degradation proceeds under unsteady state conditions with regard to terminal macroradicals, and this result is also supported by composition ratios observed for the nonvolatile oligomers. On the other hand, the value of $([TTD] + [NTTD])/[TVD]$ increases gradually with increasing time, in contrast to the results^{2c} that the corresponding composition ratios obtained for the volatile oligomers are kept constant with reaction time. The result on the nonvolatile oligomers is due mainly to a decreasing f_{TVD} value during the degradation. It is deduced from the kinetic expression^{7c} described above that the ratios between the abstraction rates of the same type of hydrogen (CH_2 or CH_3) of respective radicals differ from one another. Although the ratio $[TTD]/[NTTD]$ corresponds to the rate constant ratio between β scission rates of $R_{oi2}\cdot$, the observed value decreases gradually with reaction time. This result suggests that the reactivity for β scission depends on the segmental rotational motion of reacting radicals.

We have already examined the effects of physical factors such as the pressure in the reaction vessel and the volume and molecular weight of the matrix on the formation reactions of the volatile and nonvolatile oligomers^{7c,e}. It was made clear that the back-bitings and the intermolecular hydrogen abstractions followed by β scissions do not depend on the pressure and volume but strongly depend on the molecular weight of matrix. Thus, both the values of $[TVD]_p/[TVD]_t$ and $[TTD]_p/[TTD]_t$ of the volatile oligomers and the value of $[t\text{-Bu}]/[i\text{-Pr}]$ of the nonvolatile oligomers decrease evidently

with a decreasing molecular weight during the degradation. It could be confirmed that the decrease in molecular weight of the matrix leads to a decreasing concentration ratio of $[R_p\cdot]/[R_t\cdot]$ ^{7c,e}.

The molecular weight dependence of the ratio $[R_p\cdot]/[R_t\cdot]$ could be estimated from the composition ratios $[TVD]_p/[TVD]_t$, $[TTD]_p/[TTD]_t$, and $[t\text{-Bu}]/[i\text{-Pr}]$ and are given as^{7c,e}

$$\frac{[R_p\cdot]}{[R_t\cdot]} \propto \frac{[TVD]_p}{[TVD]_t} \propto \frac{[TTD]_p}{[TTD]_t} \propto M_n^n \quad (6)$$

$$\frac{[R_p\cdot]}{[R_t\cdot]} \propto \frac{[t\text{-Bu}]}{[i\text{-Pr}]} \propto M_n^n \quad (7)$$

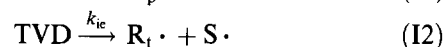
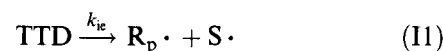
The value of exponent n could be obtained from the double logarithmic plots of equations (6) and (7) using analytical data at various reaction times. The relationships given by equations (6) and (7) were verified with a relatively high correlation for respective volatile oligomers from trimers to heptamers and the nonvolatile oligomers. The observed value of exponent n is on average, *ca.* 1.04 at 300°C and *ca.* 0.88 at 320°C for volatile oligomers^{7c}, and 1.18 at 300°C and 0.72 at 320°C for nonvolatile oligomers^{7c}. Thus, the values observed for the volatile oligomers are consistent roughly with those for the nonvolatile oligomers. Accordingly, it is clear that these oligomers are formed by different elementary reactions of the same radicals in the molten polymer matrix. In the present work, we attempt a computer simulation of the compositions of the volatile and nonvolatile oligomers, based on a complete reaction model including diffusion-controlled termination.

Reaction model

The total reaction consist of the following steps.

Initiation

(End initiation)

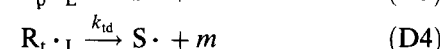
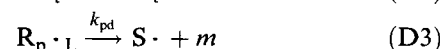
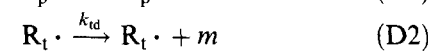
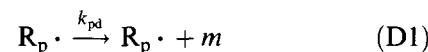


(Random initiation)

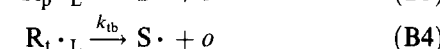
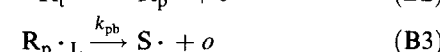
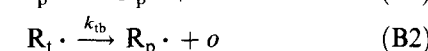
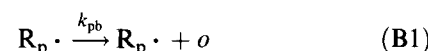


Depropagation

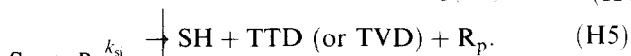
(Depolymerization, *viz.*, direct β scission)



(Back-biting followed by β scission)

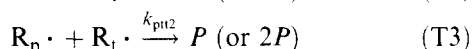
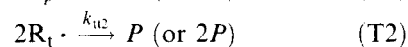
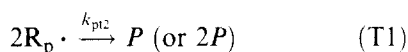


(Intermolecular hydrogen abstraction followed by β scission)

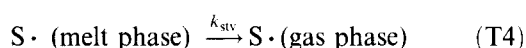


Termination

(Bimolecular termination between terminal macroradicals)



(Quasi-termination by vaporization of $S \cdot$)



In this model, $S \cdot$ is produced when the size of $R_p \cdot$ and $R_t \cdot$ just becomes volatile during depolymerization (D3 and D4) and the back-biting followed by β scission (B3 and B4), and the semi-volatile oligomers (SH) are formed by the intermolecular hydrogen abstraction of $S \cdot$ (H5 and H6). Moreover, the rates of abstractions of different types of hydrogens (CH_2 and CH_3) of $R_p \cdot$, $R_t \cdot$ and $S \cdot$ are not discriminated, and then changes of the ratios $[TTD]_p/[TVD]_p$, $[TTD]_t/[TVD]_t$, and $([TTD] + [NTTD])/[TVD]$ cannot be separately traced, and TTD and TVD of the nonvolatile oligomers are treated as a total terminal double bond (TDB), for which the functionalities f_t and f_{tn} are defined.

The rates of end initiation (I1 and I2) depend on [TTD] and [TVD], which are equal to $[P]/f_{TTD}$ and $[P]/f_{TVD}$ given by equations (3) and (4), respectively. [P] is expressed by ρ/M^{10} . The random initiation and the intermolecular hydrogen abstraction occur at any position of the main chain and, therefore, [P] should be replaced by the concentration of monomer unit [N] in the polymer. [N] is expressed by ρ/m^{10} and its value could be set to be nearly constant during the degradation¹¹, as described above. Under these conditions, the rate equations of the reactions, I1 and I2, H1 and H2, H3 and H4, and H5 and H6 are expressed, respectively, as

$$V_{ie} = k_{ie} f_t \rho / M \quad (8)$$

$$V_{ir} = k_{ir} [N] \quad (9)$$

$$V_{pi} = k_{pi} [R_p \cdot] [N] \quad (10)$$

$$V_{ti} = k_{ti} [R_t \cdot] [N] \quad (11)$$

$$V_{si} = k_{si} [S \cdot] [N] \quad (12)$$

Thus, the rate of end initiation is inversely proportional to M , and the rate of random initiation does not depend on M . On the other hand, the rate of intermolecular hydrogen abstraction depends only on the concentration of respective radicals. It was verified in the previous papers^{7c,e} that the hydrogen abstraction followed by β

scission occur under steady state conditions where the concentrations of respective on-chain macroradicals are kept low and constant and, therefore, these reactions could be represented only by the rates of the back-bittings B1 to B4 and the intermolecular hydrogen abstractions H1 to H6.

The rate equations of termination reactions T1 to T4 are written as

$$V_{pt2} = k_{pt2} [R_p \cdot]^2 \quad (13)$$

$$V_{tt2} = k_{tt2} [R_t \cdot]^2 \quad (14)$$

$$V_{prt2} = k_{prt2} [R_p \cdot] [R_t \cdot] \quad (15)$$

$$V_{stv} = k_{stv} [S \cdot] \quad (16)$$

If the rates of bimolecular terminations T1 to T3 are controlled by diffusional motion of terminal macroradicals, the rate constant k_t is governed by the frequency of encounter of two macroradicals¹² and, therefore, the diffusion coefficient D_s of macroradicals, which is related to some power of molecular weight; that is,

$$k_t = 4\pi R D N_A = K M^{-a} \quad (17)$$

where R is radius of reaction sphere and N_A is Avogadro constant. Similarly, if the rate of vaporization of $S \cdot$ (T4) is also controlled by diffusional motion of $S \cdot$, the rate constant k_{stv} may be governed by the diffusional process through the matrix, and proportional to the diffusion coefficient D_t of $S \cdot$; that is,

$$k_{stv} = 4\pi R D_t N_A = K_1 M^{-b} \quad (18)$$

The molecular weight of $S \cdot$ is smaller than that of the matrix and, thereby, its diffusional motion may be similar to tracer diffusion rather than self-diffusional motion of macroradicals¹³.

Kinetic equation

As described above, the products are mainly formed by the elementary reactions of the depropagation step (D1 to H6). The molecular weight on computation is determined by $M = mDP$, where DP is number average degree of polymerization. The rate of decrease in the volume (V) of polymer matrix corresponds to the formation rate of the volatiles including monomer and volatile oligomers, and these rates are given, respectively, as

$$-\frac{dV}{dt} = \left\{ \left(k_{pd} + k_{pb} \frac{\rho}{m} \right) [R_p \cdot] + \left(k_{td} + k_{tb} \frac{\rho}{m} \right) [R_t \cdot] \right\} \frac{V}{[N]} \quad (19)$$

$$\frac{dC}{dt} = \left\{ \left(k_{pd} + k_{pb} \frac{\rho}{m} \right) [R_p \cdot] + \left(k_{td} + k_{tb} \frac{\rho}{m} \right) [R_t \cdot] \right\} \frac{(1-C)}{[N]} \quad (20)$$

The semi-volatile oligomers are treated as part of the volatiles and their formation rate is written as

$$\frac{d[SH]}{dt} = k_{si} [S \cdot] [N] \quad (21)$$

The weight fraction (C') of SH is determined by the

equation $C' = [\text{SH}]M_{\text{SH}}V$, and C^* represents the sum of volatilization $C (= 1 - V/V_0)$ and C' .

For the volatile oligomers, the ratios $[\text{TTD}]_p/[\text{TTD}]_t$ and $[\text{TVD}]_p/[\text{TVD}]_t$ of each volatile oligomer are assumed to be represented by the observed value of $[\text{TTD}]_p/[\text{TTD}]_t$ of trimers, and the formation rates of terminal mono-olefins are given as

$$\frac{d[\text{TTD}]_p}{dt} = k_{\text{pb}}[\text{R}_p \cdot] \quad (22)$$

$$\frac{d[\text{TTD}]_t}{dt} = k_{\text{tb}}[\text{R}_t \cdot] \quad (23)$$

The concentration of polymer $[P]$ increases during the degradation, according to the equation

$$\frac{d[P]}{dt} = \left\{ \frac{(1+Y)}{2} k_{\text{pi}}[\text{R}_p \cdot] + \frac{(1+Y)}{2} k_{\text{ti}}[\text{R}_t \cdot] + \frac{Y}{2} k_{\text{si}}[\text{S} \cdot] \right\} [\text{N}] \quad (24)$$

DP can be determined by $DP = \rho/(m[P])$, because the molecular weight distribution keeps a constant value of about 2 during the degradation (Table 2). The concentration changes of respective functional groups of the nonvolatile oligomers are calculated by the equations,

$$\frac{[t\text{-Bu}]}{dt} = k_{\text{pi}}[\text{R}_p \cdot][\text{N}] \quad (25)$$

$$\frac{[i\text{-Pr}]}{dt} = k_{\text{ti}}[\text{R}_t \cdot][\text{N}] \quad (26)$$

$$\frac{[\text{TDB}]}{dt} = Y(k_{\text{pi}}[\text{R}_p \cdot] + k_{\text{ti}}[\text{R}_t \cdot] + k_{\text{si}}[\text{S} \cdot])[\text{N}] \quad (27)$$

$$\frac{[\text{NTTD}]}{dt} = (1-Y)(k_{\text{pi}}[\text{R}_p \cdot] + k_{\text{ti}}[\text{R}_t \cdot] + k_{\text{si}}[\text{S} \cdot])[\text{N}] \quad (28)$$

If the degradation reaction proceeds under steady state conditions with regard to $[\text{R}_t \cdot]$, $[\text{R}_p \cdot]$ and $[\text{S} \cdot]$, the following relationships should hold.

$$\frac{d[\text{R}_t \cdot]}{dt} = (1-X)V_{\text{ie}} + V_{\text{ir}} - V_{\text{Ltd}} - V_{\text{Ltb}} - V_{\text{tb}} - V_{\text{ti}} - V_{\text{ptt2}} - 2V_{\text{tt2}} = 0 \quad (29)$$

$$\frac{d[\text{R}_p \cdot]}{dt} = XV_{\text{ie}} + V_{\text{ir}} + V_{\text{tb}} + YV_{\text{ti}} + YV_{\text{si}} - V_{\text{Lpd}} - V_{\text{Lpb}} - (1-Y)V_{\text{pi}} - V_{\text{ptt2}} - 2V_{\text{pt2}} = 0 \quad (30)$$

$$\frac{d[\text{S} \cdot]}{dt} = V_{\text{ie}} + V_{\text{Lpd}} + V_{\text{Ltd}} + V_{\text{Lpb}} + V_{\text{Ltb}} + (1-Y)(V_{\text{pi}} + V_{\text{ti}}) - YV_{\text{si}} - V_{\text{stv}} = 0 \quad (31)$$

When respective radical concentrations are derived from equations (29) and (30), the rate of termination reaction T3 is smaller than those of the other disappearance reactions so that the rate term of reaction T3 is negligible. In such a case, the concentrations $[\text{R}_t \cdot]$, $[\text{R}_p \cdot]$ and $[\text{S} \cdot]$ are approximately obtained as

$$[\text{R}_t \cdot] = (DP)^{a/2} \times \left(\frac{1}{K_{t2}} ((1-X)k_{\text{ie}}f_i\rho(mDP)^{-1} + k_{\text{ir}}[\text{N}]) \right)^{1/2} \quad (32)$$

$$[\text{R}_p \cdot] = (DP)^{a/2} \left(\frac{[\text{R}_t \cdot]}{K_{p2}} (k_{\text{tb}} + Yk_{\text{ti}}[\text{N}] + \frac{\{\alpha(k_{\text{td}} + k_{\text{tb}}) + (1-Y)k_{\text{ti}}[\text{N}]\}k_{\text{si}}[\text{N}]}{Yk_{\text{si}}[\text{N}] + K_1(DP)^{-b}}) \right)^{1/2} \quad (33)$$

$$[\text{S} \cdot] = \{k_{\text{ie}}f_i\rho(mDP)^{-1} + (\alpha(k_{\text{pd}} + k_{\text{pb}}) + (1-Y)k_{\text{pi}}[\text{N}])[\text{R}_p \cdot] + (\alpha(k_{\text{td}} + k_{\text{tb}}) + (1-Y)k_{\text{pi}}[\text{N}])[\text{R}_t \cdot]\} \times \left(\frac{1}{Yk_{\text{si}}[\text{N}] + K_1(DP)^{-b}} \right) \quad (34)$$

Thus, these concentrations could be expressed as a function of DP .

Computation procedure

The changes in the volume of matrix and the molar concentration of each component at a given reaction time are obtained by integration of equations (19)–(28). The simultaneous differential equations are solved by the method of Runge–Kutta–Gil. For the given initial values, the radical concentrations of equations (32)–(34) are calculated using the initial DP value. The changes in volume and each molar concentration for a time interval (Δt) are calculated by the subroutine Runge–Kutta–Gil using the resulting radical concentration. These calculations are repeated in the subroutine until a given reaction time. Thus, the integrated radical concentrations are estimated as

$$[\text{R}_p \cdot] = \int [\text{R}_p \cdot] dt \cong \sum [\text{R}_p \cdot] \Delta t \quad (35)$$

$$[\text{R}_t \cdot] = \int [\text{R}_t \cdot] dt \cong \sum [\text{R}_t \cdot] \Delta t \quad (36)$$

$$[\text{S} \cdot] = \int [\text{S} \cdot] dt \cong \sum [\text{S} \cdot] \Delta t \quad (37)$$

Here, Δt is set to be 0.05 min.

In a previous paper^{7c}, we claimed that, if the termination reactions T1 to T3 are activation-controlled, the radical concentrations increase with a decreasing M during the degradation, owing to the molecular weight dependence (M^{-1}) of the end initiation given by equation (8). Then, in the present work, the two cases of termination shown in Table 4 are examined, because the quasi-termination T4 may be activation-controlled; in case I, both the bimolecular termination (T1 to T3) and the quasi-termination T4 are diffusion-controlled and, in case II, only the former is diffusion-controlled and the latter is activation-controlled. It is verified for the entangled molten polymer matrix that the value of exponent of molecular weight dependence obeying the power law is 2^{1a,13,14}. The value of exponent may be approximately 2 for the unentangled matrix, although the theoretical value of 1 is proposed when the product of D_s and zero-shear viscosity is independent of the monomeric friction factor^{13c,14}. Here, the value of 2.1 is assigned for the former; it is somewhat larger than 2.0 assigned for the latter, because the former is controlled by self-diffusional motion and the latter by tracer diffusional motion¹³. The other parameters used in the simulation are summarized in Table 5. The parameters X

and Y in the table were estimated from the ratios $[\text{TTD}]/([\text{TTD}] + [\text{TVD}])$ and $([\text{TTD}] + [\text{TVD}])/([\text{TTD}] + [\text{TVD}] + [\text{NTTD}])$ shown in Table 3, respectively. The α value was roughly assigned by fitting the C' value.

Results of simulation

A set of reasonable initial values of rate constants of reactions I1 to T4 is checked by fitting many variables such as parameters M and C^* , molar concentrations and their ratios, and functionalities of respective components. A set of kinetic constants giving a best fit is shown in Table 6. Similar values of kinetic constants are obtained when the value of 2.0 is assigned for that of the exponent b . These values listed in Table 6 are discussed later.

The results of simulation are shown in Figures 1 to 5. In all figures, the calculated values are drawn with solid or dotted lines and the observed values are plotted with marks against M_n of the nonvolatile oligomers. These figures show clearly that all of the observed values are consistently traced by the results calculated for case I rather than case II. The relationship between C^* and M_n

Table 4 Two cases examined for type of termination

Case	Value of power law exponent		Remarks ^a	
	'a' of equation (17)	'b' of equation (18)	Reactions T1-T3	Reaction T4
I	2.1	2.0	D.C.T.	D.C.T.
II	2.1	0.0	D.C.T.	A.C.T.

^a D.C.T.: Diffusion-controlled termination; A.C.T.: Activation-controlled termination

Table 5 Parameters used in simulation

Parameters	Values used
m	56
o	224 ^a
M_{SH}	800 ^b
ρ , g cm ⁻³	0.75 ^c
X	0.70 ^d
Y	0.88 ^e
α	0.20 ^f

^a Corresponds to M of tetramer

^b From ref. 7a

^c Estimated ref. 10

^d From the value of $[\text{TTD}]/([\text{TTD}] + [\text{TVD}])$

^e From the value of $([\text{TTD}] + [\text{TVD}])/([\text{TTD}] + [\text{TVD}] + [\text{NTTD}])$

^f By fitting the C' value

Table 6 A set of rate constants for best fit^a

Rate constant		(Unit)
k_{ic}	2.83×10^{-9}	(s ⁻¹)
k_{ir}	3.13×10^{-12}	(s ⁻¹)
k_{pd}	3.17×10^2	(s ⁻¹)
k_{id}	1.67×10^4	(s ⁻¹)
k_{pb}	1.67×10^2	(s ⁻¹)
k_{ib}	6.67×10	(s ⁻¹)
k_{pi}	3.33	(L · mol ⁻¹ s ⁻¹)
k_{ii}	3.33	(L · mol ⁻¹ s ⁻¹)
k_{si}	8.00×10^3	(L · mol ⁻¹ s ⁻¹)

^a Using $K_{p2} = 1.67 \times 10^{14}$ (1 mol⁻¹ s⁻¹), $K_{i2} = 2.08 \times 10^{11}$ (1 mol⁻¹ s⁻¹) and $K_1 = 8.33 \times 10^9$ (s⁻¹)

in Figure 1 is well represented by the curves obtained for case I. A marked increase of $[i\text{-Pr}]$ in a range of M_n lower than ca. 10000 in Figure 3 is fairly well traced by the simulation of case I. The agreement between the simulated and the observed values for the non-volatile oligomers results mainly from better fit of the

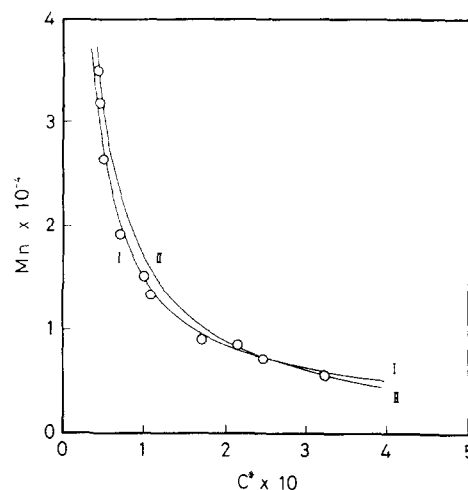


Figure 1 Plot of M_n vs. C^* , together with the calculated value drawn by solid lines

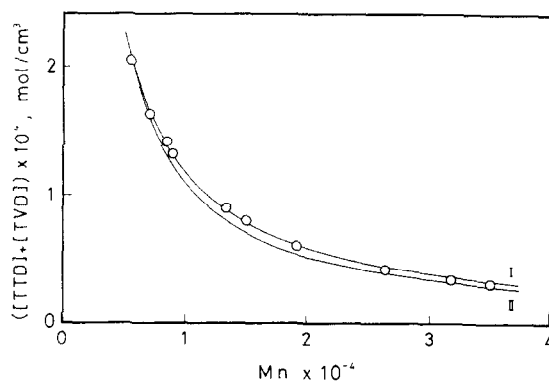


Figure 2 Plot of the concentration $[\text{TDB}]$ vs. M_n , together with the calculated value drawn by solid lines

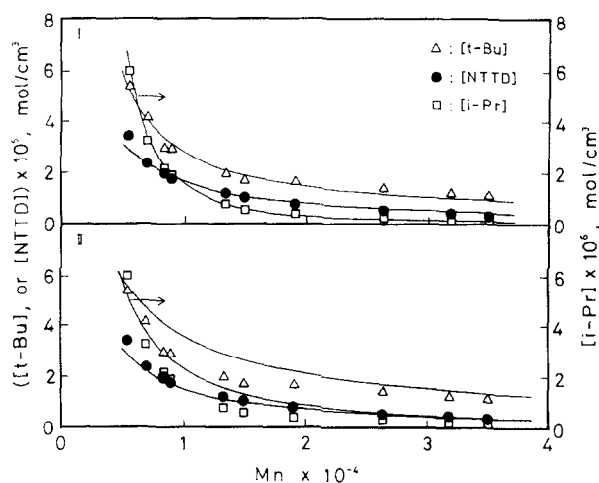


Figure 3 Plots of the concentrations $[t\text{-Bu}]$, $[i\text{-Pr}]$ and $[\text{NTTD}]$ vs. M_n , together with the calculated values drawn by solid lines

functionalities in case I, as shown in Figure 5. The changes in $[t\text{-Bu}]/[i\text{-Pr}]$ and $[\text{TTD}]_p/[\text{TTD}]_t$ for the nonvolatile and volatile oligomers correspond to that of the integrated radical concentration ratio $[\text{R}_p\cdot]/[\text{R}_t\cdot]$ (Figure 4), and their observed values are also well traced in case I. In Figure 6, the concentrations $[\text{R}_p\cdot]$, $[\text{R}_t\cdot]$ and $[\text{S}\cdot]$ calculated using equations (32) to (34) for the time interval ($\Delta t = 0.05$ min) are plotted as a function of M_n . In both cases, the concentrations of all the radicals decrease with a decreasing M_n during the degradation. It is expected at the earlier stage of reaction in case I that $[\text{R}_p\cdot]$ is larger than $[\text{S}\cdot]$. However, the order of decrement is observed as $\text{S}\cdot > \text{R}_p\cdot \gg \text{R}_t\cdot$. In a range of M_n lower than *ca.* 10 000, $[\text{R}_p\cdot]$ and $[\text{S}\cdot]$ are lower

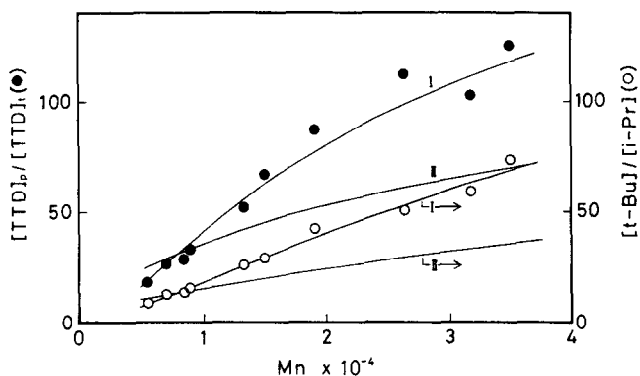


Figure 4 Plots of the values of $[\text{TTD}]_p/[\text{TTD}]_t$ and $[t\text{-Bu}]/[i\text{-Pr}]$ vs. M_n , together with the calculated values drawn by solid lines

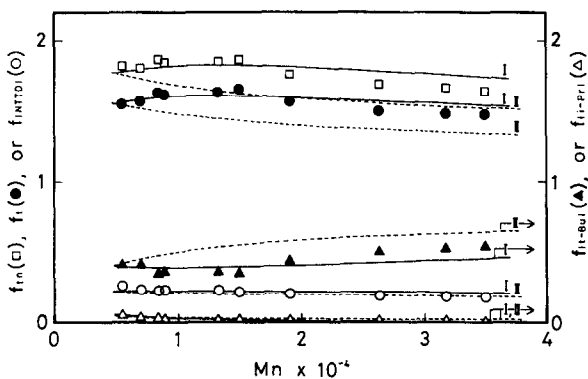


Figure 5 Plots of the functionalities of respective functional groups vs. M_n , together with the calculated values drawn by solid and dotted lines

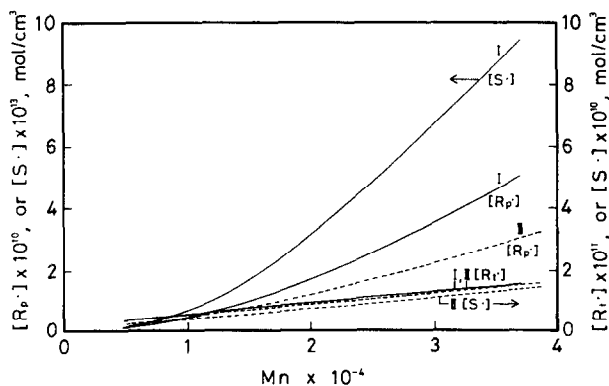


Figure 6 Relationships simulated for the concentrations $[\text{R}_p\cdot]$, $[\text{R}_t\cdot]$ and $[\text{S}\cdot]$ vs. M_n

than $[\text{R}_t\cdot]$ and, therefore, a marked increase in $[i\text{-Pr}]$ results, as shown in Figure 3. On the other hand, it would be expected in case II that $[\text{S}\cdot]$ is largest and $[\text{S}\cdot]$ as well as $[\text{R}_t\cdot]$ gradually decrease with a decreasing M_n , owing to M_n -independent quasi-termination T4. This is reflected in increasing values of f_t and f_{tn} with a decreasing M_n , as shown in Figure 5. Figure 7 shows the rate of volatilization [equation (20)] and its value per unit volume of polymer residue plotted against M_n . Both the rates decrease with a decreasing M_n and this is due to decrements of $(1 - C)$, $[\text{R}_p\cdot]$ and $[\text{R}_t\cdot]$ during the degradation. The kinetic chain length KCL is given as

$$\text{KCL} = \frac{V_{pd} + V_{td} + V_{pb} + V_{tb} + V_{pi} + V_{ti} + V_{si}}{V_{ie} + V_{ir}} \quad (38)$$

Figure 8 shows the plots of KCL vs. M_n . A larger KCL decreases more markedly with time, owing to an increasing rate of termination with a decreasing M_n during the degradation. Accordingly, it is made clear that marked decrements of $[\text{R}_p\cdot]$ and $[\text{S}\cdot]$ in case I (Figure 6) are caused by depression of the reformation rate of $\text{R}_p\cdot$ and $\text{S}\cdot$ in the depropagation step, due to a larger decrement of KCL. On the other hand, $[\text{R}_t\cdot]$ decreases slightly in spite of a large decrement of KCL, because $\text{R}_t\cdot$ is not newly generated in the depropagation step.

The molecular weight dependencies of the concentrations of respective radicals calculated using equations (32)–(34) (Figure 6) are given as

$$[\text{R}_p\cdot] \propto M_n^n \quad (39)$$

$$[\text{R}_t\cdot] \propto M_n^n \quad (40)$$

$$[\text{S}\cdot] \propto M_n^n \quad (41)$$

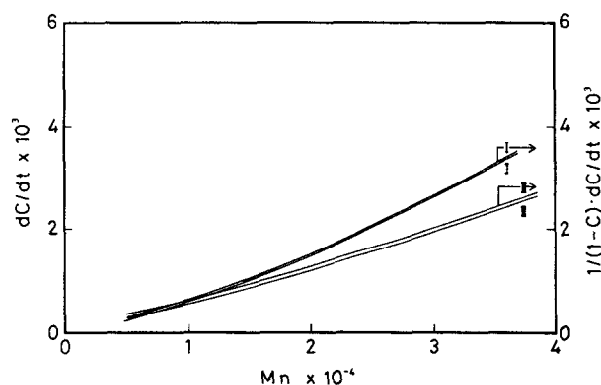


Figure 7 Relationships simulated for the volatilization rates dC/dt and $1/(1 - C) \cdot dC/dt$ vs. M_n

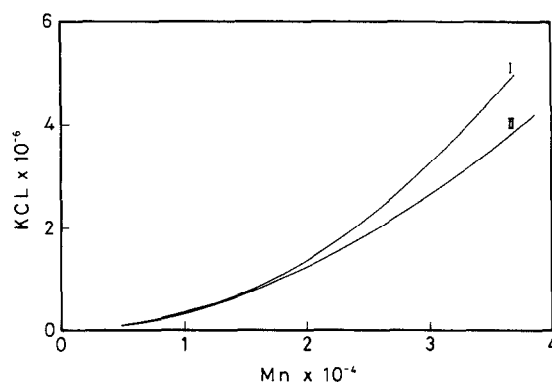


Figure 8 Relationships between the kinetic chain length KCL and M_n

Table 7 M_n dependencies of composition ratios of interest components in the nonvolatile and volatile oligomers and each radical concentration by thermal degradation of polyisobutylene ($M_n = 2.50 \times 10^5$) at 300°C

Contents	Nonvolatile oligomers		Trimers		Calculated radical concentration			
	$\frac{[t\text{-Bu}]}{[i\text{-Pr}]}$		$\frac{[\text{TTD}]_p}{[\text{TTD}]_t}$		$\frac{[\text{R}_p \cdot]}{[\text{R}_t \cdot]}$	$[\text{R}_p \cdot]$	$[\text{R}_t \cdot]$	$[\text{S} \cdot]$
n Value	1.11	1.23	1.05	1.09	1.28	2.02	0.737	2.35
Coefficient of correlation	0.9898	0.9950	0.9689	0.9880	0.9946	0.9988	0.9989	0.9962

As described above, the molecular weight dependencies of the integrated ratio $[\text{R}_p \cdot]/[\text{R}_t \cdot]$ can also be estimated from equations (6) and (7). The double logarithmic plots of equations (6), (7), (39), (40) and (41) were checked by the least square method and the values of n were determined for the observed and calculated values of $[\text{TTD}]_p/[\text{TTD}]_t$ and $[t\text{-Bu}]/[i\text{-Pr}]$ (Figure 4) and the calculated radical concentration (Figure 6) are shown in Table 7. The n value for $[\text{R}_p \cdot]/[\text{R}_t \cdot]$ corresponds to the difference between the calculated values of $[\text{R}_p \cdot]$ and $[\text{R}_t \cdot]$. In the integrated ratio $[\text{R}_p \cdot]/[\text{R}_t \cdot]$, the n values observed for the nonvolatile and the volatile oligomers agree with the calculated values. On the other hand, the n value determined from the calculated ratio $[\text{R}_p \cdot]/[\text{R}_t \cdot]$ is somewhat larger than that from the integrated ratio. The order of the molecular weight dependencies is $[\text{S} \cdot] > [\text{R}_p \cdot] \gg [\text{R}_t \cdot]$. These results could be reasonably interpreted by the reaction model consisting of the radical chain reactions of $\text{R}_p \cdot$, $\text{R}_t \cdot$ and $\text{S} \cdot$ including the diffusion-controlled termination (T1 to T4), which is governed by diffusional motion of the reacting radicals in the matrix.

Rate constants and reactivity of radicals

The rate constant of elementary reaction is related to the reactivity of the corresponding reactant or radical. A set of rate constants which was determined to satisfy the observed results is given in Table 6. Although these values are of approximate nature, the extent of occurrence of respective reactions could be evaluated by these values. For the initiation reactions (I1 to I3), the rate of end initiation reaction I1 from TTD would be nearly the same as that of the reaction I2 from TVD. If the value of frequency factor A of the scission is assumed to be about 10^{13} s^{-1} , the activation energy E_a of end initiation is estimated to be about $56.6 \text{ kcal mol}^{-1}$. Similarly, E_a for the random initiation reaction I3 is about $64.2 \text{ kcal mol}^{-1}$. The difference is about $7.8 \text{ kcal mol}^{-1}$, which is roughly consistent with the dissociation energies of the allylic C–C bond from double bond and the skeletal C–C(C)₂ bond⁵. It is found for the depolymerization reactions D1 and D3, and D2 and D4, that the rate constant k_{id} of direct β scission of $\text{R}_t \cdot$ is about 50 times larger than k_{pd} of $\text{R}_p \cdot$, and this difference corresponds to ΔE_a of about $4.5 \text{ kcal mol}^{-1}$ with $A = 10^{13} \text{ s}^{-1}$. As described above, the composition of isobutylene monomer in the volatiles increases from about 10 to 30 wt% for 15 to 300 min. The larger value of k_{id} than k_{pd} could reasonably explain that the increment of isobutylene monomer results from a marked decrease in $[\text{R}_p \cdot]$ and a gradual decrease in $[\text{R}_t \cdot]$

Table 8 Rate constants of terminations determined from equations (42)–(44)

M_n $\times 10^{-3}$	DP	Reaction T1	Reaction T2	Reaction T4
		k_{pt}^a ($\text{l mol}^{-1} \text{ s}^{-1}$)	k_{t2}^b ($\text{l mol}^{-1} \text{ s}^{-1}$)	k_{stv}^c (s^{-1})
48.5	866	2.22×10^8	1.41×10^5	1.11×10^4
5.70	102	1.01×10^{10}	1.27×10^7	8.08×10^5

^a Using $K_{p2} = 1.67 \times 10^{14} (\text{l mol}^{-1} \text{ s}^{-1})$

^b Using $K_{t2} = 2.08 \times 10^{11} (\text{l mol}^{-1} \text{ s}^{-1})$

^c Using $K_1 = 8.33 \times 10^9 (\text{s}^{-1})$

with reaction time. This result suggests that the reactivity for β scission is related to the segmental rotational motion of the reacting end radical. We will report on this problem in detail in a subsequent paper.

The back-biting reactions B1 and B3 of $\text{R}_p \cdot$ would occur somewhat predominantly than the reactions B2 and B4 of $\text{R}_t \cdot$, probably owing to a relatively lower reactivity by hyperconjugation and a steric hindrance of bulky dimethyl groups of $\text{R}_t \cdot$. Similarly, the rates of intermolecular hydrogen abstractions H1 and H2 of $\text{R}_p \cdot$ are slightly larger than those of $\text{R}_t \cdot$ (H3 and H4). However, the rates of the intermolecular hydrogen abstractions H5 and H6 of $\text{S} \cdot$ are estimated to be about 10^3 times larger than those of $\text{R}_p \cdot$ and $\text{R}_t \cdot$. This is attributable to the larger f_t value, in spite of the lower $[\text{S} \cdot]$. For the termination reactions T1, T2 and T4, the parameters K_{p2} , K_{t2} and K_1 in Table 6 are defined as

$$k_{pt2} = K_{p2}(\text{DP})^{-2.1} \quad (\text{l mol}^{-1} \text{ s}^{-1}) \quad (42)$$

$$k_{tt2} = K_{t2}(\text{DP})^{-2.1} \quad (\text{l mol}^{-1} \text{ s}^{-1}) \quad (43)$$

$$k_{stv} = K_1(\text{DP})^{-2.0} \quad (\text{s}^{-1}) \quad (44)$$

The rate constants given by equations (42)–(44) could be estimated by using the values of K_{p2} , K_{t2} and K_1 shown in the table. The values of k_{pt2} , k_{tt2} , and k_{stv} for $M_n = 4.85 \times 10^4$ ($\text{DP} = 866$) and $M_n = 5.70 \times 10^3$ ($\text{DP} = 102$) are listed in Table 8. On the other hand, the rate constant k of diffusion-controlled termination could be roughly estimated from the equation $k = 4\pi RDN_A$, by assuming the value of R ($\times 10^{-9} \text{ dm}$),

$$k = 3.78 \times 10^{16} D \quad (\text{l mol}^{-1} \text{ s}^{-1}) \quad (R = 5) \quad (45)$$

$$k = 7.56 \times 10^{17} D \quad (\text{l mol}^{-1} \text{ s}^{-1}) \quad (R = 100) \quad (46)$$

There is no information regarding the value of diffusion coefficient D at 300°C. However, the value of D of polymer molecules is in a range of about 10^{-8} to

$10^{-16} \text{ dm}^2 \text{ s}^{-1}$ in the molten polymer at a relatively lower temperature (175–215°C), depending on molecular weight and type of polymer^{13,14}. Thus, the estimated values of rate constants of termination are essentially in accordance with the observed values (Table 8). The rate of vaporization k_{stv} should be much smaller than the rate of bimolecular termination. Moreover, the value of k_{tt2} for $R_t \cdot$ is about 10^{-3} times smaller than that of k_{pt2} for $R_p \cdot$, and this suggests that bimolecular termination of $R_t \cdot$ is depressed by the steric hindrance effects. Therefore, the values of a given set of rate constants (Table 6) could be regarded as meaningful for characterization of the thermal degradation of polyisobutylene governed by self-diffusion-controlled termination.

CONCLUSIONS

The thermal degradation of polyisobutylene is characterized by the simulation using a radical chain reaction model including diffusion-controlled termination. The observed values of the volume and molecular weight of the matrix, the molar concentrations, their ratios and functionalities of main components in the products are consistently traced by this simulation. It is made clear from these results that the bimolecular termination between respective macroradicals and the vaporization of volatile radicals are controlled by the self-diffusion of reacting radicals in the molten polymer matrix. The rates of decrease are expected to be in the order $S \cdot > R_p \cdot \gg R_t \cdot$ and this results from an increase in the rate of termination with a decreasing molecular weight of the matrix polymer as the reaction proceeds.

REFERENCES

- (a) de Gennes, P. G. 'Scaling Concepts in Polymer Physics', Cornell University Press, New York, 1979; (b) Doi, M. and Edwards, S. F. 'The Theory of Polymer Dynamics', Clarendon Press, Oxford, 1986; (c) Nagasawa, M. (Ed.) 'Molecular Conformation and Dynamics of Macromolecules in Condensed System', Elsevier, New York, 1988
- Benson, S. W. and North A. M. *J. Amer. Chem. Soc.* 1959, **81**, 1139; (b) Mahadad, H. K. and O'Driscoll, K. F. *J. Polym. Sci., Polym. Chem.* 1977, **15**, 1175; (c) Horie, K. and Mita, I. *Polym. J.* 1977, **9**, 201
- (a) Horie, K. and Mita, I. *Macromolecules* 1978, **11**, 1175; (b) Mita, I., Horie, K. and Takada, M. *Macromolecules* 1981, **14**, 1428; (c) Strukelj, M., Martinho, M. G., Winnik, M. A. and Quirk, R. P. *Macromolecules* 1991, **24**, 2488
- Mita, I. and Horie, K. in 'Degradation of and Stabilization of Polymers-1' (Ed. H. H. G. Jellinek), Elsevier, New York, 1983, Chapter 5
- Mita, I. 'Aspects of Degradation and Stabilization of Polymers' (Ed. H. H. G. Jellinek), Elsevier, New York, 1978, Chapter 6
- Cameron, G. G. and Kerr, G. P. *Eur. Polym. J.* 1968, **4**, 709
- (a) Sawaguchi, T., Tekesue, T., Ikemura, T. and Seno, M. *Macromol. Chem. Phys.* 1995, **196**, 4139; (b) Sawaguchi, T., Ikemura, T. and Seno, M. *Macromol. Chem. Phys.*, 1996, **197**, 215; (c) Sawaguchi, T. and Seno, M. *Polym. J.*, 1996, **28**, 392;

- (d) Sawaguchi, T. and Seno, M. *Polymer*, 1996, **37**, 3697; (e) Sawaguchi, T., Ikemura, T. and Seno, M. *Polymer*, 1996, **37**, 5411
- Sakaguchi, Y. and Sakurada, I. *Koubunsi Kagaku* 1948, **5**, 242
- EXXON Chemical Co. Ltd., 'VISTANEX® Polyisobutylene Properties and Applications', Exxon Corporation, Houston, 1993
- (a) Cameron, G. G. *Makromol. Chem.* 1978, **100**, 255; (b) Cameron, G. G., Meyer, J. M. and McWalter, I. T. *Macromolecules* 1978, **11**, 696
- Fox, T. G. and Flory, P. J. *J. Phys. Colloid Chem.* 1951, **55**, 221
- Smoluchowski, M. *Z. Phys. Chem.* 1918, **92**, 129
- (a) Antonietti, M., Coutandin, J. and Sillescu, H. *Macromolecules* 1986, **19**, 793; (b) Green, P. F. and Kramer, E. D. *Macromolecules* 1986, **19**, 1108; (c) Nemoto, N., Kishine, M., Inoue, T. and Osaki, K. *Macromolecules* 1991, **26**, 1648
- (a) Pearson, D. S., Strate, G. V., von Meerwall, E. and Schilling, F. C. *Macromolecules* 1987, **20**, 1133; (b) Pearson, D. S., Fetters, L. J., Graessley, W. W., Strate, G. V. and von Meerwall, E. *Macromolecules* 1994, **27**, 711

APPENDIX. ABBREVIATIONS

$R_p \cdot$	Primary (p) terminal macroradical
$R_t \cdot$	Tertiary (t) terminal macroradical
$S \cdot$	Volatile small radical
$R_{oi1} \cdot$	Primary on-chain macroradical
$R_{oi2} \cdot$	Secondary on-chain macroradical
α	Molar fraction of macroradicals, yielding to $S \cdot$, $[R_p \cdot]_L/[R_p \cdot]$ and $[R_t \cdot]_L/[R_t \cdot]$
<i>t</i> -Bu	<i>Tert</i> -butyl end group, or polymer having <i>t</i> -Bu
<i>i</i> -Pr	<i>iso</i> -Propyl end group, or polymer having <i>i</i> -Pr
TTD	Terminal trisubstituted double bond, or polymer having TTD
TVD	Terminal vinylidene double bond, or polymer having TVD
TDB:	TTD + TVD
NTTD	Non-terminal trisubstituted double bond, or polymer having NTTD
(TTD) _p	Terminal mono-olefin having a TTD and a <i>t</i> -Bu formed by the back-biting of $R_p \cdot$ followed by β scission
(TVD) _p	Terminal mono-olefin having a TVD and a <i>t</i> -Bu formed by the back-biting of $R_p \cdot$ followed by β scission
(TTD) _t	Terminal mono-olefin having a TTD and a <i>i</i> -Pr formed by the back-biting of $R_t \cdot$ followed by β scission
(TVD) _t	Terminal mono-olefin having a TVD and a <i>i</i> -Pr formed by the back-biting of $R_t \cdot$ followed by β scission
P	Polymer molecules
SH	Volatiles and semi-volatile oligomers
<i>m</i>	Monomer, or its molecular weight
<i>o</i>	Volatile oligomers, or their average molecular weight
<i>K</i>	Parameter in equations (17) and (18)
<i>X</i>	Value of $[\text{TTD}]/([\text{TTD}] + [\text{TVD}])$
<i>Y</i>	Value of $([\text{TTD}] + [\text{TVD}])/([\text{TTD}] + [\text{TVD}] + [\text{NTTD}])$